



Environmental factors associated with juvenile and adult Patagonian toothfish (*Dissostichus eleginoides*) distribution around South Georgia and the South Sandwich Islands

Timothy Jones^{1,†}, Rachel D. Cavanagh^{1,*,†}, Sally E. Thorpe¹, Timothy Earl², Jennifer J. Freer¹, Simeon L. Hill¹, Oliver T. Hogg², Jaimie B. Cleeland¹, Philip R. Hollyman³, Claire M. Waluda¹, Martin A. Collins¹

¹British Antarctic Survey, NERC, Cambridge CB3 0ET, United Kingdom

²Centre of Environment Fisheries and Aquaculture Science (Cefas), Lowestoft NR33 0HT, United Kingdom

³School of Ocean Sciences, Bangor University, Askew Street, Menai Bridge, LL59 5AB, United Kingdom

*Corresponding author: British Antarctic Survey, High Cross, Madingley Road, Cambridge, CB3 0ET, United Kingdom. E-mail: rcav@bas.ac.uk

† Joint first authors

Abstract

Understanding the environmental factors driving the distribution of harvested fish species is essential for effective fisheries management, particularly in a changing climate. We investigated the spatial distribution of Patagonian toothfish (*Dissostichus eleginoides*) around South Georgia and the South Sandwich Islands, located in the rapidly changing southwest Atlantic sector of the Southern Ocean, where a commercial longline fishery for this species operates. Using scientific demersal trawl survey data, we examined environmental factors linked to the distribution of Patagonian toothfish at South Georgia, focusing on temperature and ontogenetic shifts across different developmental stages. Distribution models, informed by environmental covariates, were constructed for six size-classes (<26 cm to >66 cm total length), representing approximate annual age groups. Depth and temperature were strongly associated with distribution, with larger size-classes occupying progressively deeper habitats. Temperature relationships were evident across all size-classes, but strongest for the three smallest, with higher abundances predicted at locations where annual mean sea surface temperature exceeded 1.8°C. This suggests that spatial distribution patterns during early life stages correspond to surface temperature conditions and that this relationship persists through early growth. Adult distributions across South Georgia and the South Sandwich Islands were explored using longline fishery data. At the South Sandwich Islands, catch-per-unit-effort declined to near zero at seafloor temperatures of 0.3°C or below, coinciding with catches largely restricted to the northern part of the island chain. Overall, the results highlight strong associations between depth, temperature and Patagonian toothfish distribution, providing new insight into the timing of ontogenetic shifts and the environmental thresholds shaping spatial patterns. Understanding life stage-specific environmental sensitivities is important for improving forecasts of distributional shifts and informing fisheries management under climate change.

Keywords Southern Ocean ecosystem, species distribution models, Patagonian toothfish, ocean temperature, climate change

Introduction

The spatial distribution of marine fish is strongly influenced by environmental factors, including temperature and biogeographic boundaries (Pinsky et al. 2013), that define the conditions suitable for different species. These may vary according to age (Collins et al. 2021), maturity status (Bansemer and Bennett 2011) and body size (Collins et al. 2005, Barbeaux and Hollowed 2018). Many fish species occupy a specific thermal range determined predominantly by physiological limits (Pörtner et al. 2007, Ern et al. 2023) and modified by ecological or behavioural mechanisms (Beau-

grand and Reid 2003, Neubauer and Andersen 2019). High-latitude fish, for example, can be restricted by cold water boundaries and face habitat loss as temperatures rise (Dulvy et al. 2008, Thorson 2019, Rintz et al. 2025). In addition, deep and cold boundary zones can act as refuges or limits (Mueter and Litzow 2008, Sanderfeld et al. 2017). Understanding the environmental factors that drive the distribution of fish species is essential for fisheries management, and increasingly so in the context of climate change. Climate-driven shifts in fish distributions may lead to population declines in some areas, while in others, species may expand or be

Received: 5 December 2025. Revised: 27 February 2026. Accepted: 31 March 2026

© The Author(s) 2026. Published by Oxford University Press on behalf of International Council for the Exploration of the Sea. This is an Open Access article distributed under the terms of the Creative Commons Attribution License (<https://creativecommons.org/licenses/by/4.0/>), which permits unrestricted reuse, distribution, and reproduction in any medium, provided the original work is properly cited.

displaced from their usual ranges, presenting challenges for management (Link et al. 2011, Melbourne-Thomas et al. 2022, Cruz et al. 2024, Azmi et al. 2025).

This study explores these issues with a focus on Patagonian toothfish (*Dissostichus eleginoides*), a commercially fished notothenioid with a circumpolar distribution around islands and continental shelves in the Southern Ocean and South Atlantic, including South Georgia and the South Sandwich Islands (SSI), the focal region for this study (Fig. 1). The Patagonian toothfish population at South Georgia, neighbouring Shag Rocks, and the northern SSI, is considered a largely self-contained stock at the southern limit of the species' range, with limited connectivity to other populations (Collins et al. 2010, Arkhipkin et al. 2022, Soeffker et al. 2022). In the SSI, the southern distribution limit overlaps with the northern limit of Antarctic toothfish (*D. mawsoni*), with thermal gradients—reflecting underlying physiological differences between the species—structuring this transitional zone between sub-Antarctic and Antarctic waters (Roberts et al. 2011, Hollyman et al. 2022, Soeffker et al. 2022).

Shag Rocks, South Georgia and the SSI are part of the Scotia Arc, a predominantly submarine ridge that forms the perimeter of the Scotia Sea. Deep gaps separate these features: the South Georgia and Shag Rocks shelves (average depth \approx 200 m) are separated by a 2000 m deep canyon, and the SSI, the northernmost of which is c. 600 km southeast of South Georgia, are small and volcanically active islands with steep topography and deep-water passages ($>$ 1500 m at their deepest) between several of the islands. Regional oceanography is dominated by the eastward-flowing Antarctic Circumpolar Current (ACC) which comprises several deep-reaching ocean fronts that mark horizontal gradients in water masses and their properties (Fig. 1; Orsi et al. 1995, Park et al. 2019). Shag Rocks, located closer to the Polar Front, typically experiences warmer surface conditions than around South Georgia, which is affected more strongly by the Southern ACC Front and cooler subpolar waters, as well as glacial run off. The SSI are located south of the ACC in waters also influenced by the Weddell Sea, with a north-south gradient along the island chain in water mass properties and seasonal sea ice cover (Thorpe and Murphy 2022). There is strong intra- and inter-annual variability in the regional frontal systems (e.g. Boehme et al. 2008, Combes et al. 2023) in addition to rapid climate-driven changes, including in winds, ocean temperature, circulation, and sea ice extent and duration (Whitehouse et al. 2008, Cavanagh et al. 2021, Hogg et al. 2021).

How Patagonian toothfish will be affected by these ongoing changes is uncertain (IPCC 2019). Ontogenetic shifts in distribution are common in marine species (Wilbur 1980, Barbeaux and Hollowed 2018), with a bigger-deeper trend prevalent across multiple taxa (Macpherson and Duarte 1991) and notably for demersal scavenging species (Collins et al. 2005) such as Patagonian toothfish (Arkhipkin et al. 2003, Laptikhovskiy et al. 2006, Collins et al. 2007, 2010). The life history of this long-lived species (\sim 50 years) includes a prolonged pelagic phase during early development. Larvae then settle as small juveniles to demersal habitats in shallow waters gradually migrating deeper as they grow (Belchier and Collins 2008, Collins et al. 2010). These ontogenetic shifts result in exposure to a range of environmental conditions throughout the species' development (Cavanagh et al. 2025).

Eggs and larvae are planktonic in surface waters and therefore may be susceptible to changes in sea surface temperature (SST), which may influence planktonic duration, development rate and survival (North 2002). Retention of eggs and larvae near juvenile habitat at South Georgia and Shag Rocks is influenced by oceanographic conditions, with prevailing currents likely influencing juvenile recruitment (Brigden 2017). The smallest post-settlement fish (length $<$ 20 cm) are found mainly on the continental shelf near Shag Rocks at 100–300 m depths, adopting a primarily benthic lifestyle (Collins et al. 2007, 2010, Belchier and Collins 2008). As individuals grow, they gradually disperse to deeper water, spreading outward from their initial habitats (Collins et al. 2010). Spawning occurs annually in austral autumn and winter, typically along the South Georgia–Shag Rocks continental slope (Bamford et al. 2024, Figure 1), likely influenced by oceanographic conditions (Boucher 2018; Brigden 2017). While there is evidence of all life-stages at South Georgia, there is no indication of spawning at the SSI, such that individuals occupying the northern portion of the SSI chain may result from spill-over from South Georgia following periods of high recruitment (Soeffker et al. 2022). The lack of antifreeze proteins in Patagonian toothfish (compared to their Antarctic congener *D. mawsoni*) may limit their polewards range (Hollyman et al. 2022, Soeffker et al. 2022), with Eastman (1990) suggesting a lower temperature limit of 2°C, although individuals have since been observed at temperatures of 1.4°C (Collins et al. 2006).

Patagonian toothfish are the target species of a valuable deep-water commercial longline fishery in this region that began in the late 1980s (Agnew 2000, 2004, Collins et al. 2010). The fishery is managed domestically within the framework of the Commission for the Conservation of Antarctic Marine Living Resources (CCAMLR). The stock assessment informing the management of this fishery is an age-structured model (Earl et al. 2024, Earl and Readdy 2024) which estimates historical abundance and recruitment based on groundfish survey abundance and age composition, tag recapture rates, catch age compositions, catch-per-unit-effort (CPUE) and biological data (Masere et al. 2024). Current management is based on a 35-year projection (Constable 2000 et al. 2000) where estimates of historic recruitment inform the level and variability of future recruitment. However, in a changing environment, these baselines may not reliably predict future population dynamics (Earl et al. 2024, Ouzoulias et al. 2024, Bessell-Browne et al. 2025). Moreover, although changes in distribution and biology are monitored, environmental parameters are not explicitly included in the assessment framework (Welsford 2023).

The aim of this study is to examine how the distribution of Patagonian toothfish relates to environmental conditions from juvenile through to adult life stages, providing insights relevant to fisheries management. Specifically, species–environment models were used to identify key habitat requirements and environmental constraints, and to assess how these relationships vary with life-stage.

Methods

The analyses encompass an investigation of the distribution of early life-stages of Patagonian toothfish at South Georgia and Shag Rocks informed by scientific trawl surveys, followed by a broader

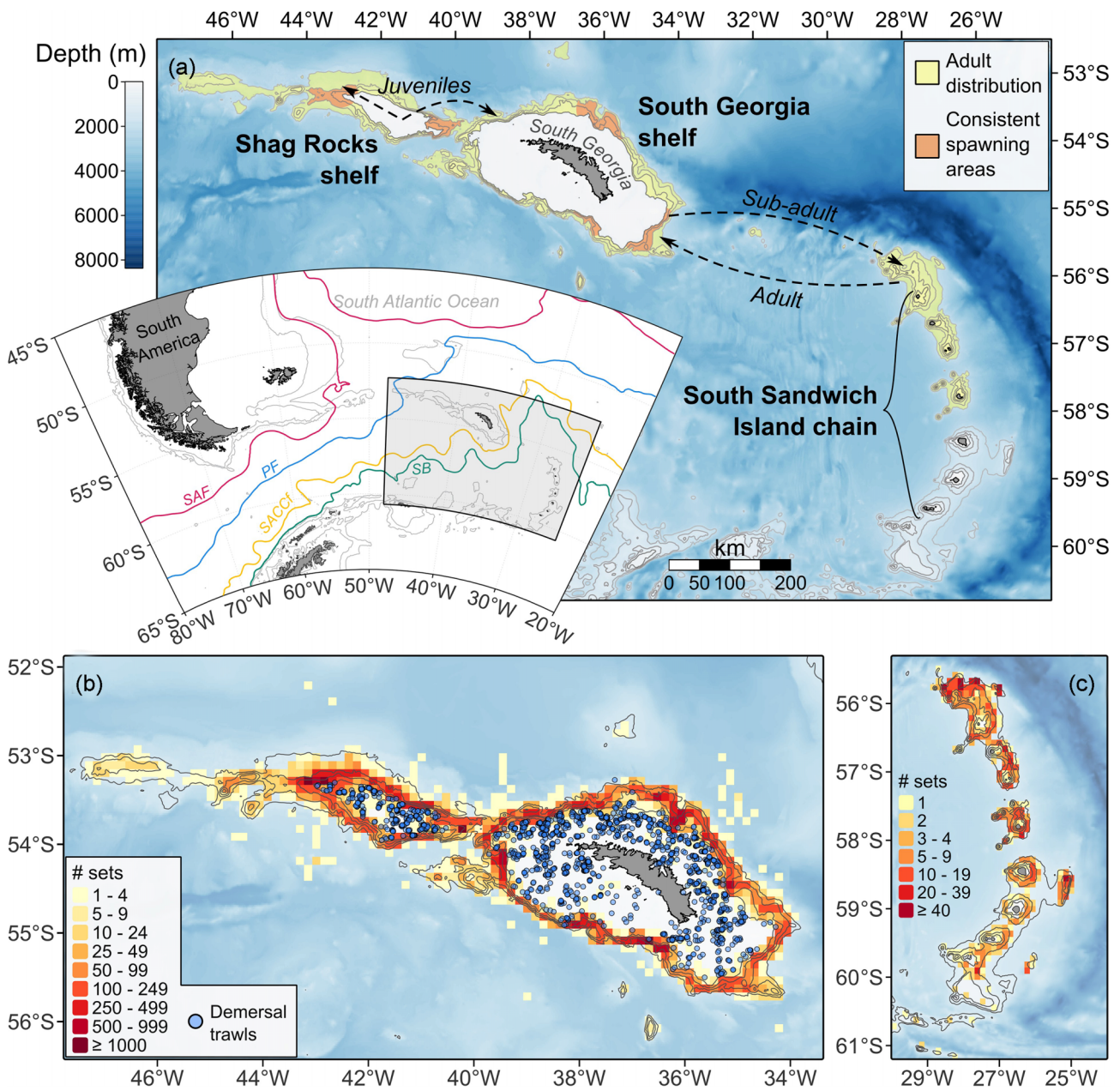


Figure 1. Maps showing the location of the study region in the Atlantic Sector of the Southern Ocean in relation to South America and major oceanographic features (SAF = Subantarctic Front, PF = Polar Front, SACC = Southern Antarctic Circumpolar Current, SB = Southern Boundary of Antarctic Circumpolar Current; Park and Durand 2019), with subsequent panels providing information on Patagonian toothfish distribution (a) and the distribution of data used in this study (b and c). The distribution of Patagonian toothfish in the study region (a) is shown for juveniles, adults, as well as the location of consistent spawning grounds (Bamford et al. 2024), and suspected ontogenetic movement between areas (Collins et al. 2010, Soeffker et al. 2022). Spatial coverage of data on Patagonian toothfish distribution is shown as the location of demersal trawls carried out during groundfish surveys (1987–2023) at South Georgia (b) and via the number of longline sets in the South Georgia (b) and South Sandwich Islands (c) longline fisheries, shown as density heatmaps (number of lines set in 10 × 10 km grid-cells). Bathymetry data shown in each panel were sourced from the ETOPO 2022 (NOAA 2022) dataset, and contour lines represent the 500, 1000, 1500, and 2000 m isobaths.

examination of adult distribution across South Georgia and SSI informed by longline fishery data (Fig. 1).

Data sources

Groundfish trawl survey data

Information collected during groundfish surveys conducted approximately biennially on the South Georgia and Shag Rocks

shelves between 1986 and 2023 (Fig. 1; see Table S1 for survey details, where S denotes figures or tables in [Supplementary materials](#)) was used to investigate the distribution of early life-stages. Sampling methods have been consistent over time, consisting of 30-minute demersal trawls (120-foot otter trawl, 18–20 m wingspread, 3–6 m headline height, 40 mm cod end mesh; Belcher 2013) at a ship speed of ~3 knots carried out between nautical twilight at dawn and dusk. Surveys were predominantly carried

Grid cells were then assigned at random to one of the 8 folds, and all trawls labelled according to the cross-validation fold assigned to the grid-cell they belonged to. Predictive accuracy was calculated using a log-likelihood score statistic equal to the summed log-likelihood of the held-out observations (one of the eight folds) given model predictions for that cross-validation fold (Dormann et al. 2018). The resulting statistic was converted to a measure D that varies from 0 to 1, with 0 indicating the model predicts no better than a null model with no spatial components (only survey and area offset terms), and 1 indicating perfect prediction (see [Supplementary materials](#) for more information on cross-validation approach). For each size class, results are presented for those models with highest predictive accuracy that also had maximum concavity (the ability of a smooth for one covariate to be approximated by other terms; Wood 2008) across covariates less than 0.7. Furthermore, given the focus on temperature effects, model statistics are also presented for those models containing temperature (one of SST, MWT, SFT) and depth covariates to examine the predictive capacity of relatively simple models for toothfish distribution.

Annual climatologies of environmental variables may not capture changes in distribution associated with varying conditions, therefore model performance was also evaluated by replacing climatological average values for each covariate (Table 2) with year-specific, or dynamic, values (see [Supplementary materials](#)).

Habitat relationships and density maps

Habitat relationships were visualised through partial dependence plots. These were created by first calculating the expected CPUE predicted by the model across the range of values exhibited by a particular habitat covariate, holding all other terms constant at their median value. Given differences in absolute abundance among size-classes, the predicted values, \hat{y} , were converted to relative density, \hat{z} , by dividing by the mean across predicted values.

$$\hat{z} = \frac{\hat{y}}{\frac{1}{n} \sum_{j=1}^n \hat{y}_j} \quad (1)$$

where n signifies the number of predicted values. Plots of relative (rather than absolute) density are therefore easier to compare given differences in CPUE among size-classes. Rather than present results for the singular best model, which may omit certain habitat covariates, an ensemble approach was used, averaging predicted relative density \hat{z} across all fitted models, weighted according to each model's log-likelihood score (see [Supplementary materials](#) for more details). This approach was applied across models, including those that did not contain the focal covariate, for which the predicted relative densities were constant (i.e. $\hat{z} = 1$) across the covariate range indicative of no effect. Therefore, the results act to show relationships for covariates included across models with higher predictive accuracy, and a flat constant relationship for non-informative terms.

Maps of toothfish density (individuals km⁻²) were created by using models to predict values onto a 2 × 2 km resolution grid populated with habitat covariates projected from their native grid. A 2 km grid was chosen to match the bathymetry data, which had the highest resolution, to best visualise distribution patterns according to bathymetric features on the South Georgia shelf. When making predictions, date was set to January-2023 so that predictions represent the most recent survey date, sun angle was set to 0.5, equal to the median value in the dataset, and area-swept was set

to 1 km² such that predicted values represented counts per km². When predicting from the models, survey random effects, which account for interannual variability in abundance, were excluded (setting exclude = "s(survey)" in the predict.gam function) such that predictions were not for any specific survey (survey effect = 0) but represented an average survey (median, given the log-link function) among those present in the dataset. As with habitat relationships, an ensemble approach to model prediction was adopted, whereby predicted maps were created for each model and then averaged, weighted by the predictive likelihood score of the corresponding model. Maps representing collective intra- and inter-model uncertainty (coefficient of variation; CV) were also created using a similar model ensemble approach. Residuals from the best model for each size-class were also checked for spatial autocorrelation. Maps showing prediction uncertainty, and results related to the assessment of spatial autocorrelation, are provided in the [Supplementary materials](#).

Broad scale analyses—adult Patagonian toothfish distribution in the Scotia Sea

Longline data analyses

Separate analyses, although founded on the same approach, were applied to catch data (response: catch weight per haul) from the South Georgia and SSI longline fishery. For each area, models were fitted to catch weight using GAMs with random effects to control for variation among vessels and years and an offset term (log(hook count)) to control for differential effort among sets. To the base model containing offset and random effects terms, we then added smooth terms for date, set depth, day of year, lunar phase, soak time, and bottom temperature to explore potential effects of each. Spatial fields, modelled via Gaussian process smoothers according to easting and northing coordinates, were also included to account for spatial variation and autocorrelation not accounted for by other model terms. Models were fitted assuming a tweedie distribution (family = tw) for catch weights as the response contained zeroes and continuous measures. Except for spatial effects that were specified using a gaussian process smoother (basis = "gp"), all remaining smooth terms were specified as thin-plate regression splines (basis = "tp"). As seafloor temperature covaries with depth and location, alternate models were fitted, varying the inclusion of depth, seafloor temperature, and spatial field to investigate whether the inclusion of depth or location confounding factors altered fitted temperature relationships. Alternate models were ranked based on Akaike's Information Criterion (AIC), and results are presented for the model with lowest AIC. Following model fitting, residuals from the best-fitting models were examined for temporal autocorrelation between catches on lines set by the same vessel each year (see [Supplementary materials](#)).

Spatial variation in CPUE and seafloor temperatures for the longline fishery areas

In addition to the analyses outlined above, spatial variation in longline catch data was visualised to identify correspondence with variation in seafloor temperatures around South Georgia and at the SSI. For each area, spatial variation in Patagonian toothfish CPUE (catch weight per 1000 hooks) was visualised by calculating the mean CPUE of all lines set within 10 × 10 km grid cells covering the extent of the longline fishery, which at the SSI ex-

tends south to where Antarctic toothfish dominate the catch (Soeffker et al. 2022). This was then compared to climatological average seafloor temperatures in each region, and by visualising temperatures across the longitudinal or latitudinal span of the South Georgia and SSI regions, respectively, at depth intervals of 1063–1246 m and 1246–1453 m, encompassing the main depths at which the fishery operates. For SSI, we also evaluated temperatures throughout the entire water column using a cross-section along a latitudinal transect along the SSI chain. Temperature data used in these analyses were obtained from the GLORYS12V1 dataset, with climatological average temperatures at the seafloor and for each depth-level (cross-section approach) calculated over data from 2005 to 2023.

Temperature trends in the Scotia Sea

To provide a large-scale overview of temperature trends throughout the known range of Patagonian toothfish in the Scotia Sea, we analysed year-average SST and water column temperatures at a range of depths for Shag Rocks, South Georgia, and the SSI chain. The SSI chain was divided into three sections to represent areas where Patagonian toothfish are frequently (northern: north of 57°S) versus rarely (southern: 58.2–60.5°S) caught by the longline fishery, with the central section (57–58.1°S) representing the transitional zone. Temperature data were obtained from the Global Ocean OSTIA (SST) and GLORYS12V1 datasets (water column temperature) for the 30-year period covering 1994 to 2023. Extracted data were cropped to the 2000 m isobath for each area (Shag Rocks = 40–44°W, South Georgia = east of 40°W), and then averaged over space and time to produce annual measures of temperature for each area for the following strata: 60–101 m (GLORYS12V1 vertical levels 20–22), 101–204 m (levels 23–26), 204–417 m (levels 27–30), 417–833 m (levels 31–34), 833–1349 m (levels 35–37), and 1349–1813 m (levels 38–39). These strata were chosen to represent putative depth ranges inhabited by Patagonian toothfish from larvae and small juvenile fish (surface, 60–101 m and 101–204 m), through intermediate-sized juveniles (204–417 m), and adults (500–2000 m). Trends in temperature were estimated for each area and depth strata by fitting a linear model with year as the independent variable using Generalised Least Squares (GLS, package nlme; Pinheiro and Bates 2025) with a first-order autoregressive correlation structure (AR1) to account for temporal autocorrelation. Trend estimates, and their uncertainty (95% confidence interval), were used to identify the areas and depth strata with the largest changes over the 1994–2023 period.

Unless otherwise specified, all analyses and data processing were performed in R version 4.3.3 (R Core Team 2024).

Results

Distribution models across toothfish size-classes at South Georgia

Spatial patterns of Patagonian toothfish abundance were consistently associated with depth and temperature across all size-classes (Table 3). In almost all instances, models containing depth and one of the three temperature covariates (mean SST; mid-water temperature at 100 m depth, MWT; seafloor temperature, SFT; Table 2) represented considerable improvements in predic-

tive accuracy compared to models only including depth (Table 3). Across all size-classes, models containing SST or MWT outperformed those containing SFT based on predictive accuracy (Table 3). Furthermore, for all size-classes the best performing model containing only temperature and depth had comparable predictive accuracy to the best performing models that contained additional habitat covariates (Table 3). Predictive accuracy scores calculated via cross-validation ranged from 0.097 (58–66 cm) to 0.410 (< 26 cm), suggesting that model predictions were accounting for ~10%–40% of the spatial variation among trawls in our dataset (Table 3).

Depending on size-class, models with highest predictive accuracy either included MWT (< 26 cm to 58–66 cm size-classes) or SST (> 66 cm size-class and total toothfish counts); however, SST and MWT were largely interchangeable and produced similar models and predictions due to the high correlation between them. Covariates associated with seabed morphology (slope and bathymetric position index) were included in the set of best models for the 26–37 cm size-class and for models of total toothfish counts but were largely absent from models for the other size-classes. Covariates associated with current speed, chlorophyll-a concentration, seafloor temperature and salinity all featured in the best predicting models across size-classes. However, none of these covariates were consistently included across size classes, or across the set of high-ranking models for a given size-class (Table 3). Notably, the best predicting models for each size-class were frequently simple, containing only two to three spatio-environmental covariates. The exceptions were for the 26–37 cm size-class model, which contained five spatio-environmental covariates, albeit with three of those related to seabed depth and morphology, and for the model fitted to total toothfish counts that contained six covariates (Table 3). However, in both cases, the addition of covariates beyond depth and temperature did not markedly improve predictive accuracy, suggesting that these additional terms were relatively weaker (Table 3).

Fitted relationships for depth were indicative of a shift towards deeper water with increasing size, shifting from depths of < 200 m (peak density at 110 m) for the < 26 cm size-class, to 200–400 m (peak density at 300 m) for 26–37 cm, and 38–47 cm fish, followed by a transition to waters > 400 m for the largest size-classes (Fig. 2). Except for the smallest and largest size-classes, which were associated with monotonically decreasing or increasing relationships with depth, respectively, size-classes displayed either a major (26–37 cm, 38–47 cm) or minor (48–57 cm) peak in abundance at ~300 m, suggesting this represents an optimum intermediate depth as toothfish grow at South Georgia (Fig. 2). The bimodal relationship estimated for 26–37 cm fish also suggests that this size-class represents the first transitional stage from very shallow depths of smaller (< 26 cm) fish to the deeper habits of larger (38–47 cm) fish (Fig. 2).

For all size classes, predicted abundances were higher at warmer SST and/or MWT, with major increases in abundance noted at SST = 1.8°C and MWT = 1.2°C for the smaller size-classes (Fig. 2). To address the uncertainty of these temperature “break-points,” functionally identified as the temperature at which relative density exceeded 0.5, or half the average density across the functions range, posterior simulations of the temperature smooth were performed (see Supplementary materials, Table S2). From these simulations, temperature “break-point” uncertainty was relatively low for the first four size-classes (95% confidence interval

Table 3. Statistics for distribution models fitted to Patagonian toothfish counts from South Georgia and Shag Rocks groundfish surveys.

Size (cm)	Depth + temperature models			Best predicting models		
	Model	edf	pD	Model	edf	pD
< 26	depth	24.6	0.251	depth + MWT	23.0	0.410
< 26	depth + SST	25.9	0.355	depth + MWT + SFT	25.7	0.408
< 26	depth + MWT	23	0.410	depth + MWT + SFT + SAL	28.6	0.407
< 26	depth + SFT	25.8	0.329	depth + curve + MWT + SFT	29.4	0.407
26–37	depth	26.3	0.017	depth + slope + BPI + MWT + SAL	42.1	0.232
26–37	depth + SST	36.4	0.18	depth + slope + BPI + MWT + SAL + VEL	44.9	0.227
26–37	depth + MWT	37.4	0.189	depth + BPI + MWT + SAL	42.2	0.226
26–37	depth + SFT	32.2	0.046	depth + slope + BPI + MWT + SFT + SAL	46.4	0.223
38–47	depth	33.0	0.041	depth + MWT + CHL	44.6	0.189
38–47	depth + SST	39.6	0.170	depth + BPI + MWT + CHL	45.6	0.187
38–47	depth + MWT	39.1	0.185	depth + MWT + CHL + VEL	47.7	0.187
38–47	depth + SFT	39.5	0.069	depth + MWT + CHL + MLT	50.4	0.186
48–57	depth	33.2	0.014	depth + MWT + VEL	38.8	0.170
48–57	depth + SST	38.4	0.129	depth + MWT	37.8	0.170
48–57	depth + MWT	37.8	0.170	depth + MWT + SAL + VEL	39.7	0.167
48–57	depth + SFT	38.6	0.105	depth + MWT + SAL	38.7	0.167
58–66	depth	30.0	0.076	depth + MWT	35.7	0.097
58–66	depth + SST	35.9	0.094	depth + MWT + SFT	32.1	0.096
58–66	depth + MWT	35.7	0.097	depth + SST	35.9	0.094
58–66	depth + SFT	33.4	0.08	depth + MWT + SFT + VEL	33.1	0.091
> 66	depth	30.4	0.107	depth + SST + SAL	34.8	0.204
> 66	depth + SST	31.8	0.193	depth + SST + MLT + SAL	35.6	0.194
> 66	depth + MWT	33.6	0.173	depth + SST	31.8	0.193
> 66	depth + SFT	37.0	-0.090	depth + BPI + SST + SAL	36.3	0.191
All	depth	34.8	-0.010	depth + slope + BPI + SST + SFT + CHL	55.7	0.188
All	depth + SST	39.6	0.182	depth + slope + BPI + SST + SFT + CHL + SAL	59.2	0.185
All	depth + MWT	39.3	0.168	depth + slope + BPI + SST + SFT + CHL + VEL	56.6	0.185
All	depth + SFT	40.4	0.081	depth + slope + BPI + SST + SFT + CHL + SAL + VEL	60.2	0.185

a: Depth is omitted in model descriptions to save on space but was included as a covariate in all models presented here

Notes: Models containing depth and a single temperature covariate are presented alongside the four best models based on predictive accuracy. Statistics are the estimated degrees of freedom (edf), and prediction accuracy score (pD) from cross-validation, which varies from 0 (no improvement over the null) to 1 (predicted values perfectly). All covariates are annual climatological mean values, unless otherwise specified, and include: sea surface temperature (SST), seafloor temperature (SFT), midwater temperature at 100 m depth (MWT), mixed layer thickness (MLT), surface salinity mean (SAL), chlorophyll-a concentration (CHL), seabed planform curvature (curve), bathymetric position index, and slope, and surface current speed (VEL).

width ranged from 0.11 to 0.28°C for SST and MWT across size-classes). However, for models fitted to the two largest size-classes there was both a shift in location of the temperature break-point to lower values, and an increase in uncertainty (95% confidence interval width from 0.20 to 0.65°C across SST and MWT), suggesting a progressive weakening in the association between distribution and near-surface temperatures with increasing size (Fig. 2).

In contrast to temperature and depth, the remaining habitat covariates displayed weaker effects (Fig. 2). Bathymetric position index (BPI) and slope were correlated with the total count, and counts of 26–37 cm toothfish suggestive of higher abundance in canyons (negative BPI, indicating locations deeper than the surrounding neighbourhood) and in shelf edge habitats (higher slope; Fig. 2). Seafloor temperature was included in the best models for the smallest size-class, 58–66 cm fish, and overall fish abundance, suggestive of an association with locations which average more than 1.3°C, with a peak at year-averaged SFT of 1.5 (< 26 cm fish) to 2°C (Fig. 2). Models for the largest and two smallest size-classes indicated a negative correlation with salinity, suggestive of higher abundance in locations with low salinity, most likely on

the South Georgia shelf (Fig. 2). A positive correlation with current speed was also evident for intermediate size-classes (38–47 cm, 48–57 cm), but the effect was relatively minor. Fitted relationships for chlorophyll-a concentration were complex and displayed a high degree of uncertainty, indicative of weak and/or location-specific effects that are not easily characterized (see Figures S4–S10 for individual model outputs for each size class).

For details on spatial autocorrelation test results, and the addition of dynamic environmental covariates to toothfish distribution models, see [Supplementary materials](#).

Size-specific predicted distributions on the South Georgia and Shag Rocks shelf

Predicted distributions resulting from these models indicate a largely restricted distribution on the Shag Rocks shelf for the < 26 cm size-class, expanding to encompass much of the Shag Rocks shelf for the 26–37 cm size-class (Fig. 3). Models also predicted higher densities in the nearshore environment and in the canyons

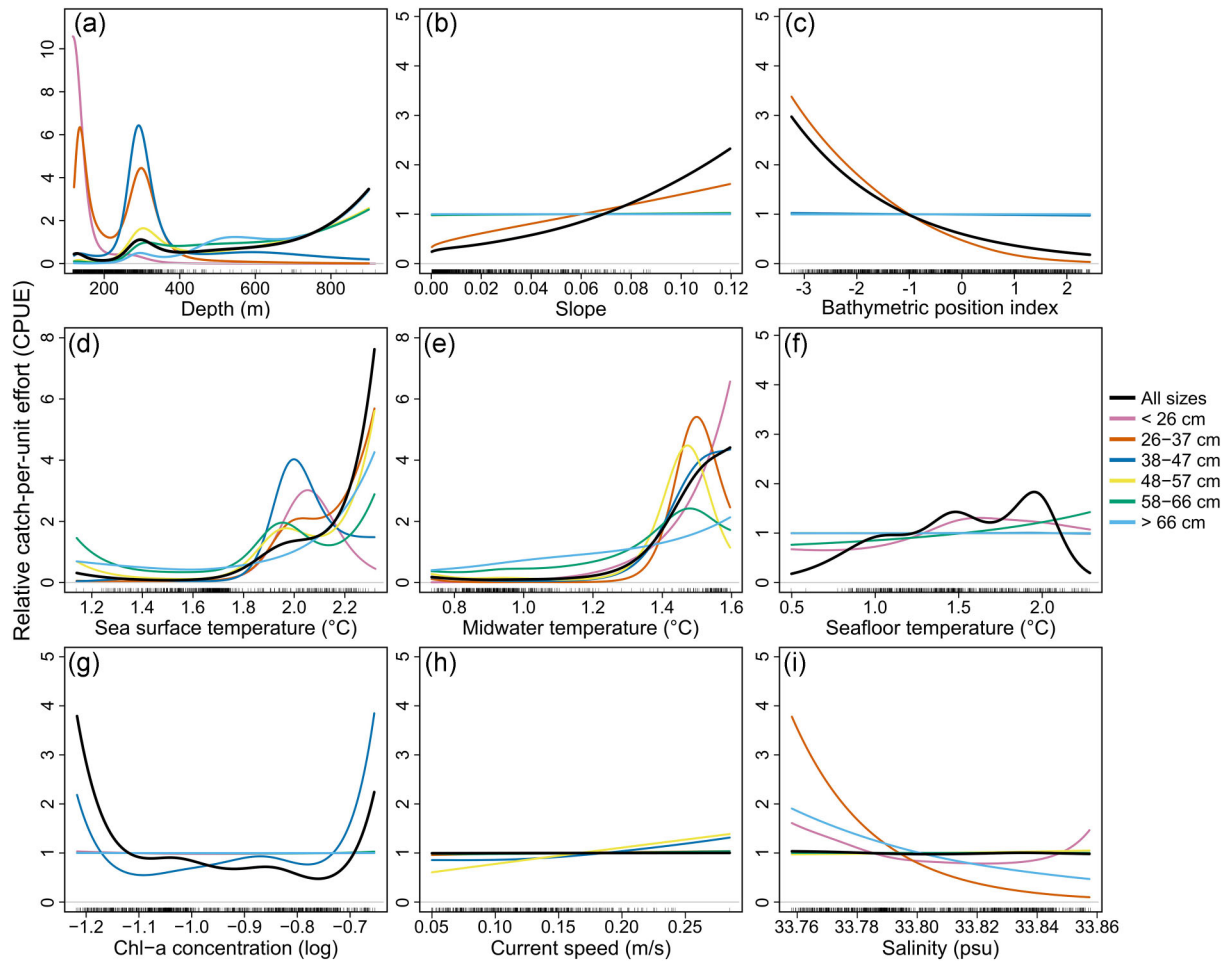


Figure 2. Model-averaged habitat covariate relationships estimated in distribution models for Patagonian toothfish at South Georgia and Shag Rocks based on demersal trawl data. Relationships are shown for covariates included in the best model for at least two size-classes and include seafloor depth (a), slope (b) and bathymetric position index (c), mean temperatures at the surface (SST; d), 100 m depth in the water column (e) and seafloor (f), and log-transformed chlorophyll-a concentration (g), current speed (h) and surface salinity (i). Values on the y-axis are relative CPUE, equal to model predicted values divided by the mean of those predictions across the covariate range, holding all other covariates constant at their median value, such that plotted values are comparable across size-classes. Apart from depth (a), SST (d) and MWT (e), y-axis scales are identical to highlight differences in effect magnitude among covariates.

around South Georgia for < 26 cm and 26-37 cm fish, respectively, which was also evident in the raw data (Fig. 3). However, nearshore areas around South Georgia have much lower, often zero, survey coverage leading to higher uncertainty (Figure S12), so we note caution when interpreting these results. Predicted distributions of 38-47 cm and 48-57 cm fish are indicative of a transition away from the Shag Rocks shelf, progressing toward the Shag Rocks shelf break, along with higher densities around the South Georgia shelf edge and in canyons extending onto the shelf (Fig. 3). Models also indicate that areas on Shag Rocks at depths of less than 300 m are devoid of the largest size-class, and that comparable densities occur off-shelf around South Georgia to those around Shag Rocks (Fig. 3). However, predicted densities remained highest at the northwest end of Shag Rocks, in addition to the eastern South Georgia shelf edge with predicted high densities of 58-66 cm fish (Fig. 3). Patterns of abundance, irrespective of size, show a bias toward Shag Rocks, with 87% of the total abundance (70-1000 m) predicted there, compared with South Georgia, where higher density areas are confined to canyons and the shelf edge (Fig. 3). However, for the two largest size-classes

caution is required when interpreting these results because the groundfish surveys only cover the shallower part (< 1000 m) of the bathymetric range of adult toothfish. Maps showing prediction uncertainty are provided in the [Supplementary materials](#) (Figure S12).

Distribution of adult Patagonian toothfish from longline data

Analyses based on CPUE of Patagonian toothfish from the South Georgia longline fishery were indicative of no meaningful effect of seafloor temperature on CPUE (Fig. 4). The fitted relationship was near constant throughout much of the temperature range (0.7–2.3°C), only varying from the mean for temperatures > 2°C (Fig. 4). This matches the observed pattern of average CPUE of no consistent change along the major west to east gradient in SFT in this region (Fig. 4). Spatial analyses did indicate the occurrence of CPUE hotspots, but these were sporadically located and seemingly unrelated to SFT (Figure S13). Analyses also indicate seasonal vari-

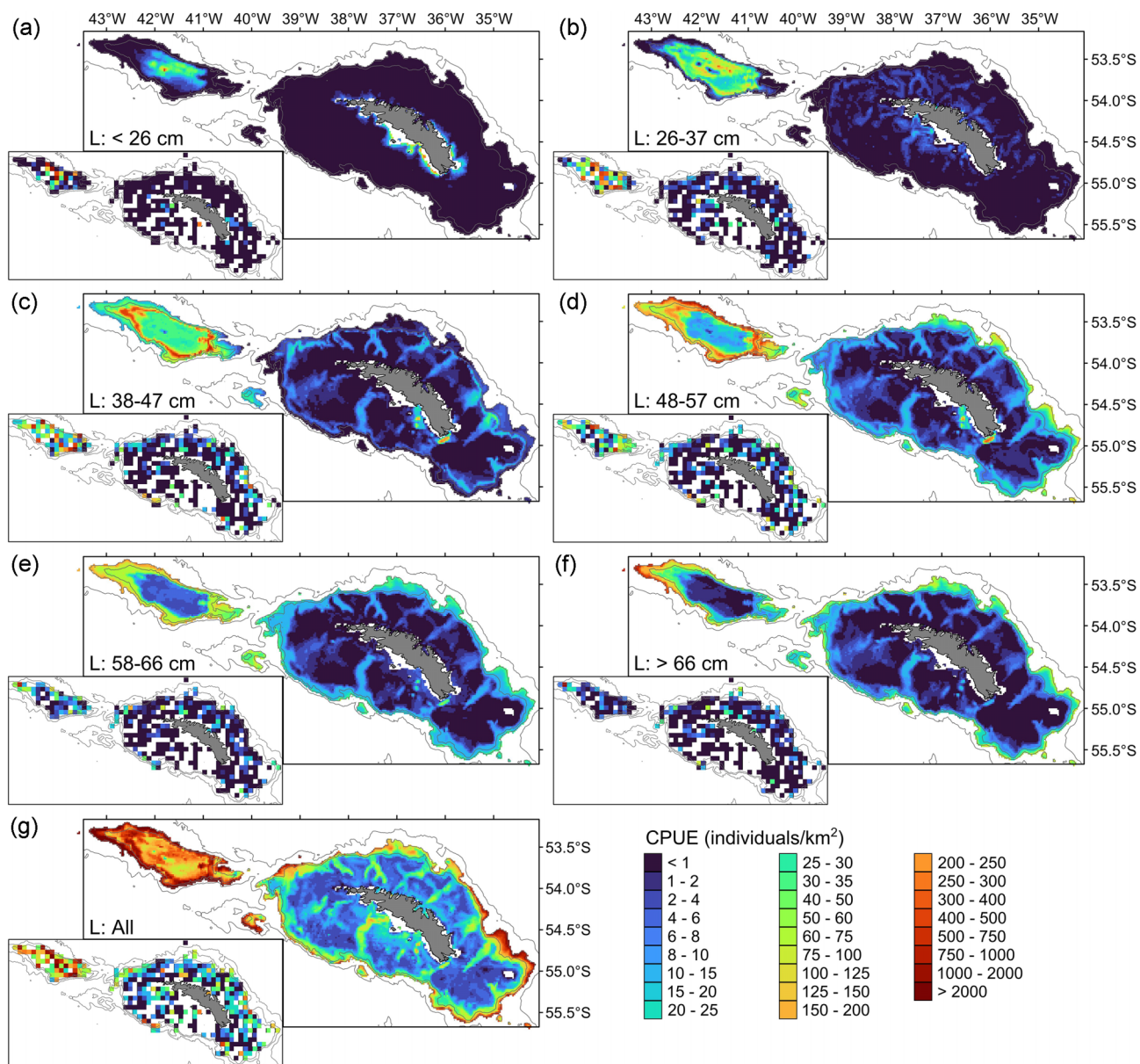


Figure 3. Model predicted densities (catch per unit effort, CPUE: individuals km^{-2}) of Patagonian toothfish for size-classes of < 26 cm (a), 26–37 cm (b), 38–47 cm (c), 48–57 cm (d), 58–66 cm (e), > 66 cm (f), and for all sizes (g) around South Georgia and Shag Rocks. Predicted distributions are shown according to fitted bathymetric and environmental relationships, with temporal covariates kept constant (date = 2023, sun angle = 0.5), and limited to seafloor depths of 70–1000 m, matching the depth range sampled during groundfish surveys. Inset maps (lower left) show the observed mean CPUE (10 km grid resolution) across all trawls for the corresponding size-class. Grey contour lines are the 500, 1000, and 2000 m isobaths.

ation in CPUE around South Georgia, with CPUE decreasing prior to/during the spawning season (June–August), as well as at depths > 1700 m (Figure S13). Catch-per-unit-effort in this region may better reflect catch efficiency than local density and this needs to be considered when interpreting these results.

At the SSI, the estimated relationship between CPUE and SFT showed a step-like transition between 0.2–0.3°C, potentially suggesting the presence of a lower thermal threshold for Patagonian toothfish in this region (Fig. 5). Examination of SFT along the SSI chain indicate that this threshold coincides with the decrease in temperature south of Saunders Island, which demarcates the division between areas where Patagonian toothfish are frequently caught (north) from those where they are seemingly ab-

sent (south) (Fig. 5). Including spatial variation in the models improved model fit based on AIC (Table S5) but obscured this temperature relationship, as it captured the same latitudinal variation in CPUE while also better capturing CPUE hotspots in the northern part of the SSI chain (Figure S14). Despite that, a step-like temperature effect was still evident in that model, reaching an approximate asymptote at 0.2°C (Fig. 5). Plotted results for the seafloor temperature relationships are shown for models with and without spatial fields (Fig. 5B), but full results inclusive of all model terms, are given in the Supplementary materials (Figure S14 and S15). Latitudinal gradients in temperature at the main depths where the fishery operates (1063–1453 m) indicate that temperatures vary little with latitude across the northern (0.3–0.5°C) and southern (0.1–

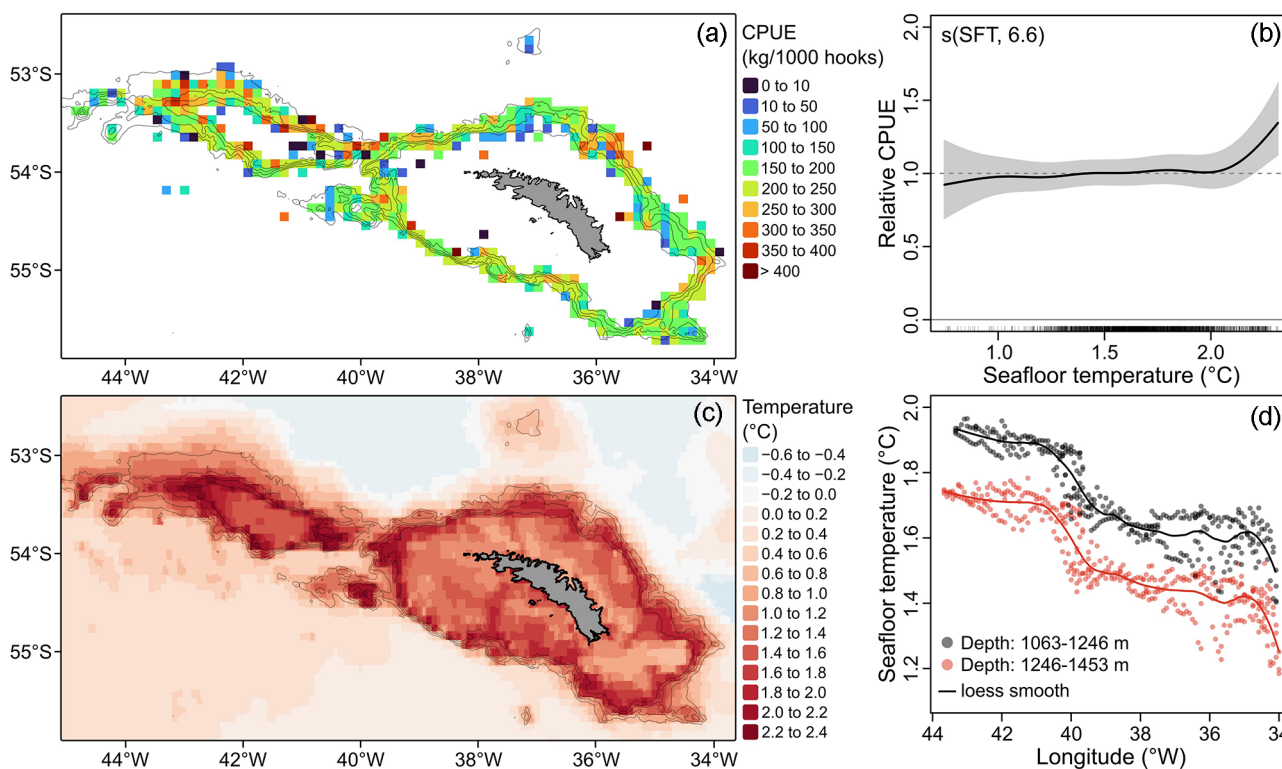


Figure 4. Distribution of Patagonian toothfish CPUE from longline catch data in relation to sea floor temperature at South Georgia. The mean CPUE (a) across all lines set between 2005 and 2023 per 10 km grid cell is shown to indicate broad-scale distribution. The relationship between CPUE and sea floor temperature (b) for the South Georgia longline fishery from a Generalised Additive Model is shown as the mean and 95% confidence interval (shading) of the estimated relationship scaled to relative CPUE by dividing by the mean fitted value across the function's range. Spatial variation in sea floor temperatures is plotted as a map (c) and according to longitude (d) for sea floor depth intervals of 1063–1246 m and 1246–1453 m around the South Georgia and Shag Rocks shelf edge, corresponding to main depths targeted by the fishery. Values plotted in (c) and (d) represent climatological annual mean temperatures from 2005 to 2023 extracted from the Global Ocean Physics Reanalysis dataset.

0.3°C) portions of the SSI chain but decrease by 0.2°C between the two areas (Fig. 5). While temperatures north of Saunders Island are warmer, therefore more favourable for Patagonian toothfish, their lower occurrence further south may also be linked to the two deep-water passages north and south of Saunders Island (Fig. 5). In both passages, average temperatures near the sea floor are below 0°C, which may inhibit transit between the two areas (Fig. 5). In addition to temperature and spatial variation, the analyses of longline catch data also indicated that CPUE increased between 2009 and 2013, followed by a declining trend from 2013 onward (Figure S14).

Results regarding temporal autocorrelation between catches on subsequent lines set by the same vessel within a fishing season are provided in the [Supplementary materials](#).

Temperature trends across the Patagonian toothfish range in the Scotia Sea

Over the last 30 years (1994–2023) SST increased in each area examined, with trend estimates varying from 0.07°C/decade (95% CI: –0.03 to 0.18) in the southern part of the SSI chain to 0.17°C/decade (95% CI: 0.05 to 0.28) at South Georgia (Fig. 6). While warming trends were evident for most sub-surface depth strata, temperatures appeared to have remained stable or cooled over the same time-period at depths of 223–454 m and 110–223 m,

respectively (Fig. 6). Further examination of temperature at those depth strata indicated relatively higher interannual variability, along with a non-linear trend through time with temperatures decreasing from 2005–2007 relative to pre-2005 levels, followed by static (SSI) or increasing trends (South Georgia, Shag Rocks) (Figure S17). Whilst temperatures at these depths may not be relevant to Patagonian toothfish in the SSI, given the presumption of a largely adult population, the relatively higher interannual variability is suggestive of less predictable conditions for juvenile toothfish at South Georgia. At depths > 454 m, a near constant warming trend of 0.04–0.05°C/decade was observed in all regions (Fig. 6), suggesting widespread warming conditions throughout the adult Patagonian toothfish range in the Scotia Sea. However, we note caution when interpreting these trends as analyses of subsurface temperatures are based on model reanalysis (GLO-RYS12V1) and while this incorporates in-situ measurements, the corresponding outputs may be subject to shifting biases through time.

Discussion

Overall, the findings of this study provide support for depth- and temperature-associated relationships in the distribution of Patagonian toothfish, offering new insight into the nature and timing of ontogenetic shifts and potential environmental drivers and

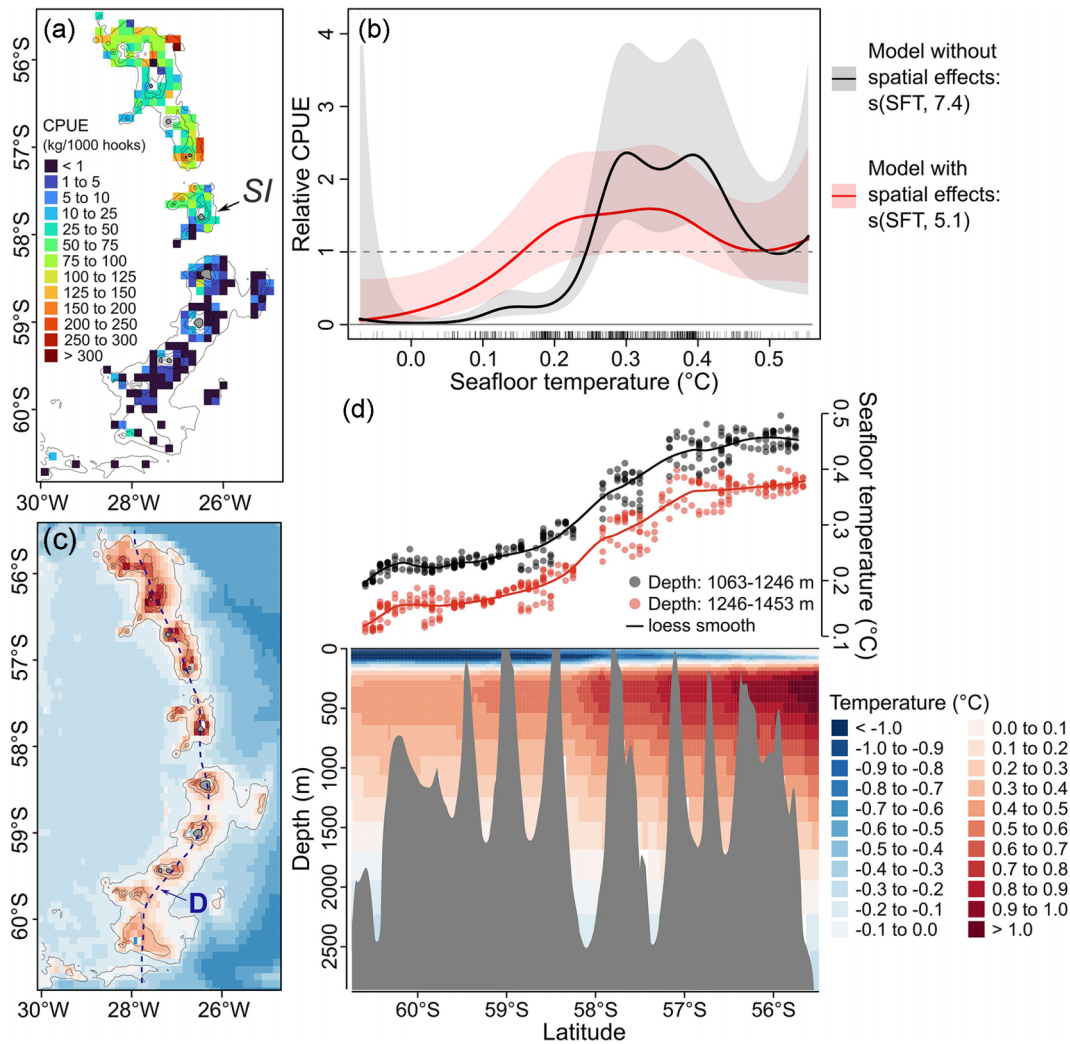


Figure 5. Patagonian toothfish distribution in relation to temperature along the South Sandwich Islands (SSI) chain. Spatial distribution of Patagonian toothfish (a) is shown via the mean CPUE across all lines set between 2009 and 2023 per 10 km grid cell. Saunders Island (SI), referred to in the main text, is also shown. The relationship between CPUE and seafloor temperature (b) for the SSI longline fishery from Generalised Additive Models with and without spatial effects are shown as the mean and 95% confidence interval (shading) of the estimated relationship scaled to relative CPUE by dividing by the mean fitted value across the function's range. Temperatures at the seafloor (c) and throughout the water column (d) along a transect spanning the SSI chain (dashed line in c) are also shown and represent climatological annual mean temperatures from 2009 to 2023 extracted from the Global Ocean Physics Reanalysis dataset.

thresholds shaping spatial patterns. Most analyses of marine thermal niches focus on adult life stages, largely because data for other stages are limited. In this study, temperature relationships were examined across different developmental stages to explore life stage-specific environmental sensitivities, providing a basis for improving forecasts of distributional changes and informing fisheries management in a changing climate.

Ontogenetic shifts in distribution and association with environmental factors

The distribution of Patagonian toothfish measuring less than 37 cm suggested an association with depths less than 200 m (< 26 cm) to 400 m (26–37 cm) during the first two years of life. Similar ontogenetic shifts in vertical distribution have been documented for Patagonian toothfish on the Patagonian shelf (Lee et al.

2024), suggesting that changes in depth distribution may be similar across populations. When combined with an apparent lower temperature limit of 1.8°C at the surface, or 1.2–1.4°C at 100 m depth, this corresponded to a highly constrained predicted distribution, largely on the Shag Rocks shelf. A preference for shallower habitats in juvenile fish has been documented across multiple species (Gibson et al. 2002, Munsch et al. 2016, Perry et al. 2018) and may be associated with factors such as avoidance of predation risk, ontogenetic changes in foraging behaviour, or warmer temperatures (Sheaves et al. 2015). Recent analyses suggest that juvenile Patagonian toothfish abundance on the Shag Rocks shelf covaries with temperature during and following spawning, with lower abundance following cooler years (Cavanagh et al. 2025). This finding, coupled with the result from the present study that juvenile distribution is associated with temperature, aligns with evidence that temperature may be most limiting during early development (Collin et al. 2021). In general, fish larvae are assumed

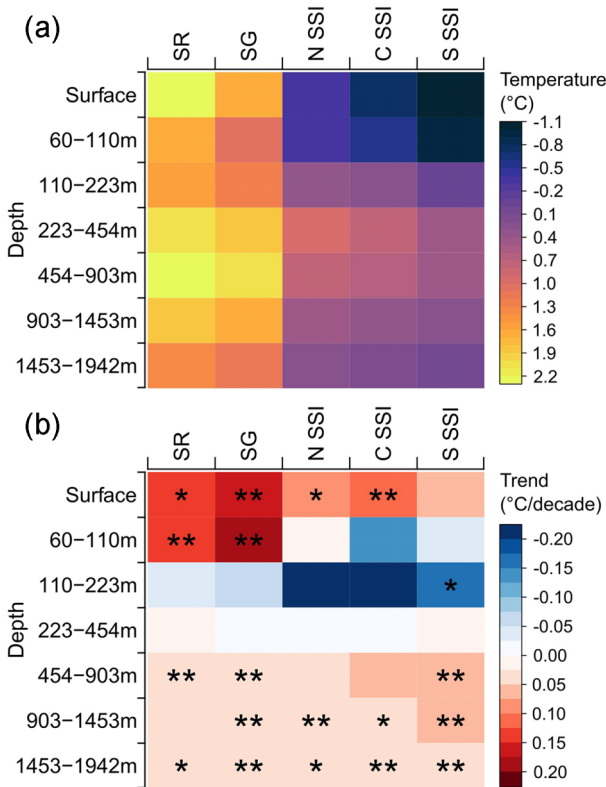


Figure 6. Long-term average temperature (a) and trend estimates (b) for regions and depth-strata inhabited by Patagonian toothfish in the Scotia Sea. Average temperatures (a) represent the mean temperature from 1994–2023 within the 2000 m isobath in each region (Shag Rocks = 40–44°W, South Georgia = east of 40°W, N SSI = north of 57°S, C SSI = 57–58.1°S, S SSI = 58.2–60.5°S) at the stated depth range. Temperature trends (°C/decade; b) are from a linear model fitted to year-average temperatures for the same spatial (horizontal and vertical) and temporal extents as described in (a). Trend significance is shown as either * or **, based on whether the 90% (*) or 95% (**) confidence interval of the trend estimate didn't overlap with 0. All data were obtained from the Copernicus Marine Data Store, with sea surface temperature (SST) extracted from the Global Ocean OSTIA SST dataset, and remaining data extracted from the Global Ocean Physics Reanalysis dataset.

to be more temperature sensitive than juveniles or adults (Moyano et al. 2017), and the association with temperature exhibited by the smallest size-classes of Patagonian toothfish may reflect a carry-over from larval development. Larvae may preferentially occur in, or exhibit higher survivability, in warmer waters. As such, variability in environmental conditions may amplify fluctuations in the abundance of early life-stages through time (Cavanagh et al. 2025), as there are limited alternative areas of suitable habitat to act as refugia if conditions are suboptimal at this “hotspot” on the Shag Rocks shelf.

However, the temperatures associated with juvenile Patagonian toothfish distribution broadly correspond to the division between Shag Rocks and the South Georgia shelf, suggesting that temperature may act as a proxy for underlying biogeographic (e.g. alternate prey) or other oceanographic (e.g. salinity, productivity) differences between the two areas. Notably, the ichthyofaunal assemblage on the South Georgia shelf is more diverse with relatively higher densities of predatory fish such as Scotia-Sea ice-

fish (*Chaenocephalus aceratus*) and South Georgia icefish (*Pseudochaenichthys georgianus*) (Belchier 2013, Gregory et al. 2017), which may prey upon juvenile toothfish. In contrast, the smaller-bodied yellowfin notothen (*Patagonotothen guntheri*) dominate, and are restricted to, the Shag Rocks shelf and are primary prey for juvenile toothfish (Collins et al. 2007, 2008). However, these differences are also likely tied to temperature, with yellowfin notothen occurring in warmer waters from the southern Patagonian shelf to Shag Rocks (Collins et al. 2008), and icefish species (apart from mackerel icefish, *Champscephalus gunnari*, which inhabit both areas; Fallon et al. 2016) potentially unable to withstand the warmer temperatures at Shag Rocks (Beers and Jayasundara 2015).

Whilst the two smallest size-classes (< 26 cm, 26–37 cm) were predominantly caught on the Shag Rocks shelf, they were also captured in lower numbers on the South Georgia shelf, mainly in the nearshore environment (Fig. 2). It is possible that juvenile toothfish are more abundant in shallow nearshore areas around South Georgia than suggested by the models, as these areas are largely unsuitable for trawl sampling. However, any associated bias regarding spatial distribution and relation to temperature is likely minimal given that larger size-classes, found at greater depths more accessible to trawl sampling, display similar temperature relationships (i.e. Figure 2d).

The relationship between abundance and SST or MWT was largely the same for Patagonian toothfish up to the 38–47 cm size-class (around the first three years of age), which all appeared to inhabit locations within a similar temperature range (SST > 1.8°C), prior to a shift to encompass a wider range of temperatures at larger sizes. As noted above in the context of the results for the smallest size-class, temperature conditions during early development potentially influence areas of suitable habitat for later stages. In the larger size-classes (≥ 48 cm), the observed temperature relationship, which indicates higher densities in warmer locations, albeit at much reduced rates compared to smaller size-classes, may be an artefact of individuals remaining on the Shag Rocks shelf near initial settlement grounds. This is particularly so given that larger sized individuals occur in deeper water (Collins et al. 2010), and are therefore not exposed to surface conditions. This also aligns with other research indicating that realized or observed thermal niches of marine organisms are determined during early development (Collin et al. 2021, Drost et al. 2015). The observed weakening relationship with SST and MWT with increasing size (≥ 48 cm) is likely a consequence of downslope migration facilitating dispersal away from Shag Rocks to areas around South Georgia given the deepwater canyon (>1500 m) separating the two areas, with only larger fish migrating across. However, an association with seafloor temperatures > 1.5°C, with an optimum of 2°C was also evident for the 38–47 cm and 48–57 cm size-classes (Fig. 2). Whether this is an artefact of the depth range inhabited (seafloor temperatures typically increase up to a maximum of ~2°C at 600 m; Fig. 4), or an attempt to remain within a specific temperature range is difficult to disentangle. For the largest size-class, associations with temperature were much reduced, aligned with the hypothesis that thermal ranges widen from early developmental stages through to adults (Dahlke et al. 2020, Collin et al. 2021).

Across all size classes, the observed spatial distribution patterns can be conceptualized in terms of three connected, non-exclusive processes: depth-related habitat use and ontogenetic shifts; biogeographic differences and prey/predator assemblages

(including differences in ichthyofaunal communities between areas); and temperature, which may influence distribution both directly through physiological effects and indirectly as an integrative proxy for underlying spatial and environmental gradients. The relative influence of these processes likely varies across ontogeny, with juvenile distributions potentially reflecting depth preferences, prey availability, and early-life thermal conditions, while larger size-classes may remain near initial settlement grounds or migrate downslope, contributing to the observed weakening of temperature associations with increasing size. We note that, although the models captured consistent spatial associations, some of the observed spatial variation remained unexplained, likely reflecting factors not explicitly represented, such as fine-scale ecological interactions, localized hydrographic features, and behavioural processes.

Broad-scale distribution of adults in relation to seafloor temperature

Results from the longline fishery catch data from around South Georgia indicate limited influence of seafloor temperature on CPUE. This is not unexpected given that most areas in the depth range targeted by the fishery had seafloor temperatures of 1–2.5°C, therefore a lower temperature threshold may not occur within this region. In addition, because adult fish are vulnerable to longline fishing (700–2000 m), this will also influence their apparent distribution, making environmental effects more difficult to assess than for smaller fish caught in the groundfish survey.

At SSI, adult Patagonian toothfish abundance declined rapidly below temperatures of 0.3°C, suggesting a threshold for their distribution. Whether this is a genuine temperature threshold is uncertain, as multiple non-exclusive hypotheses may give rise to the same latitudinal gradient in Patagonian toothfish CPUE.

The first of these is that an annual average temperature of 0.3°C represents the limit below which Patagonian toothfish are unable to sustain core functions (Sandersfeld et al. 2017). This is consistent with their lack of antifreeze glycoproteins preventing them from occupying sub-zero temperatures (Miya et al. 2015). Whilst a physiological explanation is compelling, Patagonian toothfish have been captured throughout the SSI chain—albeit at much reduced rates in the south (i.e. Figure 5)—suggesting that some individuals can survive at lower temperatures, at least over short periods of time.

A second hypothesis is that the observed distribution is truncated due to the biogeographic boundary imposed by deep-water passages north and south of Saunders Island, which happen to coincide with the 0.3°C threshold. In both passages, temperature at depth is below 0°C and midwater current velocities are high, indicating that transit near or above the seafloor may be prevented by temperature conditions (seafloor), transverse current velocity (midwater), or a combination thereof.

Finally, the distributional limit may be due to competition with Antarctic toothfish, potentially mediated by ambient temperature conditions (Kordas et al. 2011). Longline catches along the SSI chain transition from Patagonian toothfish in the north, to Antarctic toothfish south of Saunders Island (Soeffker et al. 2022), indicating opposite abundance trends. Antarctic toothfish are a high-Antarctic species adapted to sub-zero temperatures (Chen and Cheng 1997), with a preferred range of -0.1 to 0.06°C (Nissen et

al. 2025). They may exclude Patagonian toothfish in the colder southern part of the SSI chain (and vice versa further north), suggesting the 0.3°C temperature threshold reflects competitive balance between the species. Supporting this is the observation that Antarctic toothfish have expanded northward during recent years (Soeffker et al. 2022), coincident with a reduction in the Patagonian toothfish population (Figure S14–15), implying that Antarctic toothfish can occupy sub-optimal, warmer habitats when competition is reduced. Extending this reasoning, this suggests that distributional limits of both species at SSI may be linked to pulses of Patagonian toothfish recruitment at South Georgia (Soeffker et al. 2022), with a more southerly boundary following periods of high recruitment and spill-over of juveniles to the SSI, followed by a gradual reduction in Patagonian toothfish and northward expansion of Antarctic toothfish in the years between high Patagonian toothfish recruitment.

Determining whether the apparent temperature threshold at SSI reflects physiological limits, bathymetric boundaries, prey and predator assemblages, and/or altered competitive dynamics will require further study. A further consideration is that the longline analyses have data limitations, including that information on factors such as specific gear type or the potential influence of cetacean depredation was not available for inclusion. While their omission is unlikely to affect the broad patterns identified here, these factors are known to affect longline catch rates (Soeffker et al. 2014, Abreu et al. 2024) and warrant consideration in future studies.

This study provides new insights into factors associated with Patagonian toothfish distribution and also highlights remaining uncertainties for future work to address, including knowledge gaps for early life stages, biogeographic influences, and predator-prey interactions. These could be further explored by combining environmentally focused approaches with biogeographic frameworks (e.g. Nissen et al. 2025, Rintz et al. 2025) and considered in the context of ongoing and projected changes in the regional physical environment.

Implications for fisheries management

Several key considerations emerge from these findings for fisheries management. Reliance on fishery-dependent data focused on adults risks overlooking early-life bottlenecks or habitat constraints influencing population structure. Evaluating only adult distribution underestimates vulnerability to factors such as temperature change and misses critical early-life habitat. Here, analysis based solely on adults would reveal only the potentially lower thermal limit at SSI, without identifying Shag Rocks as a possible “thermal island” for juveniles. This perspective is essential for revealing early-year distribution changes and highlighting areas important for recruitment and sensitive to environmental change. Identifying and monitoring juvenile habitats, especially thermal refuges, is critical for understanding recruitment dynamics and population resilience under climate change (Barceló et al. 2016, Stamp et al. 2025).

Incorporating early life-stage information into management considerations will improve the accuracy of forecasting and the effectiveness of management. Knowledge gaps remain, particularly for eggs and larval stages, including vertical distribution, retention and dispersal (Cavanagh et al. 2025). Fisheries management needs to be flexible and responsive, accounting for climate-driven

changes—including in temperature and habitat availability—that differentially affect life stages and geographic areas, rather than treating populations as environmentally homogenous.

Acknowledgements

We acknowledge the UK Government Darwin Plus Programme for funding this project. We thank the British Antarctic Survey (BAS) and the UK Government funded Blue Belt Programme for providing additional support. We thank the crews, vessel owners, scientists and observers involved in the groundfish surveys and the Commission for the Conservation of Antarctic Marine Living Resources (CCAMLR) for permission to use longline fishery data (under CCAMLR Data Request 660). This study was conducted using E.U. Copernicus Marine Service Information (OSTIA sea surface temperature, <https://doi.org/10.48670/moi-00165>; GLORYS12V1 full depth temperature; <https://doi.org/10.48670/moi-00021>).

Author contributions

Timothy Jones (Conceptualization [lead], Formal Analysis [lead], Methodology [lead], Visualization [lead], Writing—original draft [lead]), Rachel D. Cavanagh (Conceptualization [lead], Funding acquisition [lead], Project administration [lead], Supervision [lead], Writing—original draft [lead]), Sally Thorpe (Conceptualization [supporting], Writing—review & editing [equal]), Timothy Earl (Writing—review & editing [equal]), Jennifer Freer (Writing—review & editing [equal]), Simeon Hill (Writing—review & editing [equal]), Oliver T. Hogg (Writing—review & editing [equal]), Jaimie B. Cleeland (Writing—review & editing [supporting]), Philip Richard Hollyman (Writing—review & editing [supporting]), Claire Waluda (Writing—review & editing [supporting]), Martin Collins (Conceptualization [supporting], Writing—review & editing [equal]).

Supplementary material

Supplementary material is available at *ICES Journal of Marine Science* online.

Conflicts of interest

The authors declare that there were no conflicts of interest in this study

Funding

The project was funded by the UK Government Darwin Plus Programme (DPLUS189). R.C., M.C., J.F., S.H., S.T., C.W. were additionally supported by the BAS Ecosystems programme “Research, Conservation and Leadership in Southern Ocean Ecosystems (CONSEC),” funded by the Natural Environment Research Council National Capability Science (Antarctic Logistics and Infrastructure) programme.

Data availability statement

The groundfish survey data are available from the UK Polar Data Centre <https://doi.org/10.5285/fd2f9f1c-bb9f-484e-bbc1-b3d20668b8d2> (Collins et al. 2026). The longline fishery data is available by request to the CCAMLR Secretariat. The OSTIA and GLORYS12V1 temperature products used in this study are publicly available from the E.U. Copernicus Marine Service Information (<https://doi.org/10.48670/moi-00165>, <https://doi.org/10.48670/moi-00021>).

References

- Abreu J, Hollyman PR, Xavier JC *et al.* Trends in population structure of Patagonian toothfish over 25 years of fishery exploitation at South Georgia. *Fish Res* 2024;**279**:107122. <https://doi.org/10.1016/j.fishres.2024.107122>
- Agnew DJ. The illegal and unregulated fishery for toothfish in the Southern Ocean, and the CCAMLR catch documentation scheme. *Mar Policy* 2000;**24**:361–74. [https://doi.org/10.1016/S0308-597X\(00\)00012-9](https://doi.org/10.1016/S0308-597X(00)00012-9)
- Agnew DJ. *Fishing South: History and Management of South Georgia Fisheries. Government of South Georgia and the South Sandwich Islands.* St. Albans: The Penna Press, 2004, 128pp.
- Arkipkin A, Brickle P, Laptikhovsky V. Variation in the diet of the Patagonian toothfish with size, depth and season around the Falkland Islands. *J Fish Biol* 2003;**63**:428–41. <https://doi.org/10.1046/j.1095-8649.2003.00164.x>
- Arkipkin AI, Brickle P, Lee B *et al.* Taxonomic re-appraisal for toothfish (*Dissostichus*: notothenioidea) across the Antarctic Polar Front using genomic and morphological studies. *J Fish Biol* 2022;**100**:1158–70. <https://doi.org/10.1111/jfb.15013>
- Azmi K, Pilling G, Bell J *et al.* Putting Regional Fisheries Management Organisations’ Climate Change House in Order. *Fish and Fisheries* 2025;**26**:1040–7. <https://doi.org/10.1111/faf.70015>
- Bamford C, Hollyman PR, Abreu J *et al.* Spatial, temporal, and demographic variability in Patagonian toothfish (*Dissostichus eleginoides*) spawning from twenty-five years of fishery data at South Georgia. *Deep Sea Res Part I.* 2024;**203**:104199. <https://doi.org/10.1016/j.dsr.2023.104199>
- Bansemmer CS, Bennett MB. Sex-and maturity-based differences in movement and migration patterns of grey nurse shark, *Carcharias taurus*, along the eastern coast of Australia. *Mar Freshwater Res.* 2011;**62**:596–606. <https://doi.org/10.1071/MF10152>
- Barbeaux SJ, Hollowed AB. Ontogeny matters: climate variability and effects on fish distribution in the eastern Bering Sea. *Fisheries Oceanography*, 2018;**27**:1–15. <https://doi.org/10.1111/fofg.12229>
- Barceló C, Ciannelli L, Olsen EM *et al.* Eight decades of sampling reveal a contemporary novel fish assemblage in coastal nursery habitats. *Global Change Biol* 2016;**22**:1155–67. <https://doi.org/10.1111/gcb.13047>
- Beaugrand G, Reid PC. Long-term changes in phytoplankton, zooplankton and salmon related to climate. *Global Change Biol*, 2003;**9**:801–17. <https://doi.org/10.1046/j.1365-2486.2003.00632.x>
- Beers JM, Jayasundara N. Antarctic notothenioid fish: what are the future consequences of ‘losses’ and ‘gains’ acquired during long-term evolution at cold and stable temperatures? *J Exp Biol*, 2015;**218**:1834–45. <https://doi.org/10.1242/jeb.116129>

- Fallon NG, Collins MA, Marshall CT *et al.* Assessing consistency of fish survey data: uncertainties in the estimation of mackerel icefish (*Champscephalus gunnari*) abundance at South Georgia. *Polar Biology* 2016;**39**:593–603. <https://doi.org/10.1007/s00300-015-1810-0>
- Gibson RN, Robb L, Wennhage H *et al.* Ontogenetic changes in depth distribution of juvenile flatfishes in relation to predation risk and temperature on a shallow-water nursery ground. *Marine Ecology Progress Series* 2002;**229**:233–44. <https://doi.org/10.3354/meps229233>
- Gregory S, Collins MA, Belchier M. Demersal fish communities of the shelf and slope of South Georgia and Shag Rocks (Southern Ocean). *Polar Biology*, 2017;**40**:107–21. <https://doi.org/10.1007/s00300-016-1929-7>
- Hijmans R. raster: geographic Data Analysis and Modeling. 2025. R package version 3.6-31, <https://rspatial.org/raster> (1 October 2024, date last accessed)
- Hogg OT, Cavanagh RD, Grant S *et al.* Key climate change effects on the coastal and marine environment around the Polar UK Overseas Territories. *Marine Climate Change Impacts Partnership Science Review*. 2021 <https://doi.org/10.14465/2021.orc02.pol>
- Hollyman PR, Hill SL, Laptikhovskiy VV *et al.* A long road to recovery: dynamics and ecology of the marbled rockcod (*Notothenia rossii*, family: nototheniidae) at South Georgia, 50 years after overexploitation. *ICES J Mar Sci* 2021;**78**:2745–56. <https://doi.org/10.1093/icesjms/fsab150>
- Hollyman PR, Soeffker M, Roberts J *et al.* Bioregionalization of the South Sandwich Islands through community analysis of bathyal fish and invertebrate assemblages using fishery-derived data. *Deep Sea Res Part II* 2022;**198**:105054. <https://doi.org/10.1016/j.dsr2.2022.105054>
- Ilich A, Misiuk B, Lecours V *et al.* MultiscaleDTM: an open-source R package for multiscale geomorphometric analysis. *Transactions in GIS* 2023;**27**:1164–204. <https://doi.org/10.1111/tgis.13067>
- Kordas RL, Harley CD, O'Connor MI. Community ecology in a warming world: the influence of temperature on interspecific interactions in marine systems. *J Exp Mar Biol Ecol*, 2011;**400**:218–26. <https://doi.org/10.1016/j.jembe.2011.02.029>
- Laptikhovskiy V, Arkhipkin A, Brickle P. Distribution and reproduction of the Patagonian toothfish *Dissostichus eleginoides* Smitt around the Falkland Islands. *J Fish Biol* 2006;**68**:849–61. <https://doi.org/10.1111/j.0022-1112.2006.00973.x>
- Lee B, Skeljo F, Randhawa HS *et al.* Early life-history patterns in Patagonian toothfish *Dissostichus eleginoides* from the Patagonian Shelf. *Marine Ecology Progress Series* 2024;**726**:131–48. <https://doi.org/10.3354/meps>
- Lellouche JM, Greiner E, Bourdalle-Badie R *et al.* The Copernicus Global 1/12° Oceanic and Sea Ice GLORYS12 Reanalysis. *Frontiers in Earth Science* 2021;**9**:698876. <https://doi.org/10.3389/feart.2021.698876>
- Link JS, Nye JA, Hare JA. Guidelines for incorporating fish distribution shifts into a fisheries management context. *Fish and Fisheries*, 2011;**12**:461–9. <https://doi.org/10.1111/j.1467-2979.2010.00398.x>
- Macpherson E, Duarte CM. Bathymetric trends in demersal fish size: is there a general relationship? *Marine Ecology Progress Series*, 1991;**71**:103–12. <https://doi.org/10.3354/meps071103>
- Marra G, Wood SN. Practical variable selection for generalized additive models. *Comput Stat Data Anal*, 2011;**55**:2372–87. <https://doi.org/10.1016/j.csda.2011.02.004>
- Masere C, Le Clech R, Alewijnse S *et al.* Consideration of the impact of tagging and recapture effort on mark-recapture abundance estimators within integrated Casal2 stock assessments. 2024. CCAMLR Working Group on Statistics, Assessments and Modelling WG-SAM-2024/22.
- Melbourne-Thomas J, Audzijonyte A, Brasier MJ *et al.* Poleward bound: adapting to climate-driven species redistribution. *Reviews in Fish Biology and Fisheries* 2022;**32**:231–51. <https://doi.org/10.1007/s11160-021-09641-3>
- Miya T, Gon O, Mwale M *et al.* Multiple independent reduction or loss of antifreeze trait in low Antarctic and sub-Antarctic notothenioid fishes. *Antarct Sci* 2015;**28**:17–28. <https://doi.org/10.1017/S0954102015000413>
- Moyano M, Candebat C, Ruhbaum Y *et al.* Effects of warming rate, acclimation temperature and ontogeny on the critical thermal maximum of temperate marine fish larvae. *PLoS One* 2017;**12**:e0179928. <https://doi.org/10.1371/journal.pone.0179928>
- Mueter FJ, Litzow MA. Sea ice retreat alters the biogeography of the Bering Sea continental shelf. *Ecol Appl*, 2008;**18**:309–20. <https://doi.org/10.1890/07-0564.1>
- Munsch S, Cordell J, Toft J. Fine-scale habitat use and behaviour of a nearshore fish community: nursery functions, predation avoidance, and spatiotemporal habitat partitioning. *Marine Ecology Progress Series*. 2016;**557**:1–15. <https://doi.org/10.3354/meps11862>
- Neubauer P, Andersen KH. Thermal performance of fish is explained by an interplay between physiology, behaviour and ecology. *Conservation Physiology*, 2019;**7**:coz025. <https://doi.org/10.1093/conphys/coz025>
- Nissen C, Caccavo JA, Morée AL. Twenty-First-Century Environmental Change Decreases Habitat Overlap of Antarctic Toothfish (*Dissostichus mawsoni*) and Its Prey. *Global Change Biol*, 2025;**31**:e70063. <https://doi.org/10.1111/gcb.70063>
- NOAA. ETOPO 2022 15 Arc-Second Global Relief Model. NOAA National Centers for Environmental Information. 2022. <https://doi.org/10.25921/fd45-gt74>
- North AW. Larval and juvenile distribution and growth of Patagonian toothfish around South Georgia. *Antarct Sci*, 2002;**14**:25–31. <https://doi.org/10.1017/S0954102002000548>
- Orsi AH, Whitworth T, Nowlin WD. On the meridional extent and fronts of the Antarctic Circumpolar Current. *Deep Sea Res Part I*, 1995;**42**:641–73. [https://doi.org/10.1016/0967-0637\(95\)00021-W](https://doi.org/10.1016/0967-0637(95)00021-W)
- Ouzoulias F, Massiot-Granier F, Alewijnse S *et al.* Effects of implementing dynamic B0 in toothfish fisheries. 2024. CCAMLR Working Group on Statistics, Assessments and Modelling WG-SAM-2024/25.
- Park Y-H, Durand I. Altimetry-derived Antarctic Circumpolar Current fronts. SEANOE, 2019. <https://doi.org/10.17882/59800>
- Park Y-H, Park T, Kim T-W *et al.* Observations of the Antarctic Circumpolar Current over the Udintsev Fracture Zone, the narrowest choke point in the Southern Ocean. *J Geophys Res: Oceans* 2019;**124**:4511–28. <https://doi.org/10.1029/2019JC015024>
- Perry D, Staveley TAB, Gullström M. Habitat Connectivity of Fish in Temperate Shallow-Water Seascapes. *Frontiers in Marine Science* 2018;**4**:440. <https://doi.org/10.3389/fmars.2017.00440>

- Pinheiro J, Bates D. nlme: linear and Nonlinear Mixed Effects Models. 2025. R package version 3.1-167. <https://CRAN.R-project.org/package=nlme> (1 October 2024, date last accessed)
- Pinsky ML, Worm B, Fogarty MJ *et al.* Marine taxa track local climate velocities. *Science* 2013;**341**:1239–42. <https://doi.org/10.1126/science.1239352>
- IPCC. IPCC Special Report on the Ocean and Cryosphere in a Changing Climate. Portner HO, Roberts DC, Masson-Delmotte V, Zhai P, Tignor M, (eds.), *et al.*, (eds.), **2019**, 2019. <https://www.ipcc.ch/srocc/>
- Pörtner HO, Peck L, Somero G. Thermal limits and adaptation in marine Antarctic ectotherms: an integrative view. *Philosophical Transactions of the Royal Society B: Biological Sciences*, 2007;**362**:2233–58. <https://doi.org/10.1098/rstb.2006.1947>
- Rintz CL, Koubbi P, Ramiro-Sánchez B *et al.* Biogeographical Regions and Climate Change: lanternfishes Shed Light on the Role of Climatic Barriers in the Southern Ocean. *Global Change Biol* 2025;**31**:e70256. <https://doi.org/10.1111/gcb.70256>
- Roberts J, Xavier JC, Agnew DJ. The diet of toothfish species *Dissostichus eleginoides* and *Dissostichus mawsoni* with overlapping distributions. *J Fish Biol*, 2011;**79**:138–54. <https://doi.org/10.1111/j.1095-8649.2011.03005.x>
- Sandersfeld T, Mark FC, Knust R. Temperature-dependent metabolism in Antarctic fish: do habitat temperature conditions affect thermal tolerance ranges? *Polar Biology*, 2017;**40**:141–9. <https://doi.org/10.1007/s00300-016-1934-x>
- Sheaves M, Baker R, Nagelkerken I *et al.* True Value of Estuarine and Coastal Nurseries for Fish: incorporating Complexity and Dynamics. *Estuaries Coasts* 2015;**38**:401–14. <https://doi.org/10.1007/s12237-014-9846-x>
- Soeffker M, Hollyman PR, Collins MA *et al.* Contrasting life-history traits of two toothfish (*Dissostichus* spp.) species at their range edge around the South Sandwich Islands. *Deep Sea Res Part II* 2022;**201**:105098. <https://doi.org/10.1016/j.dsr2.2022.105098>
- Stamp T, West E, Stewart JE *et al.* Effective protection of essential fish habitat requires understanding fish spatial ecology—lessons learnt from protected European bass nursery areas. *ICES J Mar Sci* 2025;**82**:fsaf035. <https://doi.org/10.1093/icesjms/fsaf035>
- Thorpe SE, Murphy EJ. Spatial and temporal variability and connectivity of the marine environment of the South Sandwich Islands, Southern Ocean. *Deep Sea Res Part II*, 2022;**198**:105057. <https://doi.org/10.1016/j.dsr2.2022.105057>
- Thorson JT. Measuring the impact of oceanographic indices on species distribution shifts: the spatially varying effect of cold-pool extent in the eastern Bering Sea. *Limnol Oceanogr*, 2019;**64**:2632–45. <https://doi.org/10.1002/lno.11238>
- Welsford D. Summary and Recommendations from Independent review of CCAMLR toothfish assessments. 2023. SC-CAMLR-42/02 Rev. 2
- Whitehouse MJ, Meredith MP, Rothery P *et al.* Rapid warming of the ocean around South Georgia, Southern Ocean, during the 20th century: forcings, characteristics and implications for lower trophic levels. *Deep Sea Res Part I* 2008;**55**:1218–28. <https://doi.org/10.1016/j.dsr.2008.06.002>
- Wilbur HM. Complex life cycles. *Annu Rev Ecol Syst* 1980;**11**:67–93. <https://www.jstor.org/stable/2096903>
- Wood SN. Fast stable restricted maximum likelihood and marginal likelihood estimation of semiparametric generalized linear models. *Journal of the Royal Statistical Society Series B: Statistical Methodology* 2011;**73**:3–36. <https://doi.org/10.1111/j.1467-9868.2010.00749.x>

Handling editor: Olav Rune Godø